Roland Würschum*, Robert Weitenhüller, Robert Enzinger and Wolfgang Sprengel

Modulated dilatometry as a tool for simultaneous study of vacancy formation and migration

https://doi.org/10.1515/ijmr-2022-0022
Received January 19, 2022; accepted April 1, 2022;
published online July 21, 2022

Abstract: A model is presented to derive both vacancy formation and migration characteristics from length change measurements upon modulated time-linear heating. The length variation with linear heating yields access to the equilibrium concentration of thermal vacancies. The modulation amplitude and the phase shift between modulated temperature and length change is determined by the ratio of equilibration rate and modulation frequency which yields access to the vacancy migration characteristics. The contribution from thermal lattice expansion is obtained from a reference measurement at high modulation frequencies. Compared to static isothermal equilibration measurements after temperature jumps, the processes are monitored under quasi-equilibrium conditions avoiding obstacles associated with fast temperature changes. Furthermore, in contrast to the static isothermal case where the equilibration rate is obtained from the time-exponential decay, its determination from the amplitude and phase shift of modulation offers higher precision. The method is suitable for materials with high thermal vacancy concentrations and low vacancy diffusivities, among which is the important class of intermetallic compounds with B2-structure.

Keywords: Kinetic model; Modulated dilatomtry; Thermal vacancy formation; Vacancy equilibration; Vacancy migration.

1 Introduction

The principle of dilatometry, i.e., of measuring volume changes caused by physical or chemical processes, dates back to the nineteenth century [1]. Meanwhile, dilatometry has developed to a powerful toolbox with a number of measurement routines applicable to various phenomena in materials science. A major application field of dilatometry is the study of *transformation and precipitation processes* in alloys [2–7]. Owing to recent progress in sensitivity and long-term stability by using a specially designed highly stable non-contact dilatometer [8], this application route could be extended to the most application-relevant class of Al alloys with low amounts of Mg and Si [9, 10] (for review see [11]).

Dilatometry is further successfully applied to study *defect annealing phenomena* in sub-microcrystalline metals after severe plastic deformation yielding access to grain boundary excess volume [12, 13]. In the same manner the concentration of deformation-induced excess vacancies became measurable by dilatometry for ultrafine-grained Ni [14–16]. With dilatometry as a function of orientation, even anisotropic behaviour of vacancy annealing, which arises from structural anisotropy in this material, could be measured allowing conclusions regarding the vacancy formation and relaxation volume [14].

The fundamental idea of detecting *thermal vacancies* in metals by macroscopic length change measurements goes back to Feder and Nowick [17]. They compared the length change obtained from the macroscopic measurement with that from X-ray diffraction in order to subtract the contribution from thermal lattice expansion for estimating the contribution from thermal vacancies to the overall macroscopic length change. Based on this principle, but measuring macroscopic length change and X-ray diffraction simultaneously on the same sample, Simmons and Balluffi [18] could successfully determine thermal vacancy concentrations, which was later further refined by Hehenkamp et al. [19].

For a high vacancy concentration and low vacancy diffusivity as observed, e.g., in various intermetallic compounds, both the vacancy formation and migration can be studied by isothermally monitoring the length change after a temperature jump [20, 21]. From the time dependence of the length change, the vacancy equilibration time constant, and from its amplitude the difference in thermal vacancy concentration upon temperature jump

***Corresponding author: Roland Würschum**, Institute of Materials Physics, Graz University of Technology, Petersgasse 16, 8010 Graz, Austria, E-mail: wuerschum@tugraz.at. https://orcid.org/0000-0003-4624-4433
Robert Weitenhüller, Robert Enzinger and Wolfgang Sprengel, Institute of Materials Physics, Graz University of Technology, Graz, Austria

can be deduced. The inherent advantage of the method is that isothermal monitoring of the length change is not affected by thermal lattice expansion. Disadvantages, however, associated with the required temperature jump are potential defect losses during cooling and transient phemonena affecting the measuring accuracy right after sudden temperature change.

These disadvantages can be avoided by monitoring the vacancy processes by temperature-modulated time-linear heating, which is the concept proposed in the present work. Upon time-linear heating, the temperature-dependence of the thermal vacancy concentration can be monitored in thermal equilibrium, rather than upon step-like temperature change. The superimposed temperature modulation allows monitoring of the temperature-dependence of the vacancy equilibration under conditions near to equilibrium. As will become clear in the forthcoming, the modulation is also the essential key for determining the contribution from thermal lattice expansion without the necessity of another technique.

The modulation model presented in the following makes dilatometry a powerful tool for simultaneous study of vacancy formation and migration for a wide spectrum of alloys exhibiting high vacancy concentrations and low vacancy diffusivities. Although the model is elaborated for dilatometry, the concept is not restricted to length change measurements, but applicable to other defect-sensitive techniques as well.

Dilatometric measurement techniques and temperature modulated thermal analysis including their various applications are reviewed by James et al. [22] and by Kraftmakher [23]. The latter also discusses temperature modulated dilatometry, however, mainly describing various experimental setups for assessing instantaneous thermal expansion coefficients. Aspects of analysing kinetic processes using temperature modulated dilatometry have so far only been addressed scarcely, e.g., in specific applications related to second order phase transitions [24], to processes in polymers [25], or to coating/substrate interaction [26]. To our knowledge there have been no applications up to now of temperature modulated dilatometry for the study of vacancy formation and migration processes as proposed in the present article.

2 Model

We consider vacancies in thermal equilibrium with the concentration $C_V(T)$ as function of temperature T

$$C_{V,eq}(T) = \exp\left(\frac{S_V^F}{k_B}\right)\exp\left(-\frac{H_V^F}{k_B T}\right) \tag{1}$$

where k_B denotes the Boltzmann constant, and H_V^F and S_V^F the vacancy formation enthalpy and entropy, respectively. Any deviation $\Delta C_V = C_V - C_{V,eq}$ from the equilibrium concentration $C_{V,eq} = C_{V,eq}(T_0)$ at a given temperature T_0 gives rise to equilibration, which can be described by the rate equation

$$\frac{dC_V(t)}{dt} + \frac{C_V(t) - C_{V,eq}}{\tau} = 0 \tag{2}$$

with the equilibration rate [21]

$$\frac{1}{\tau} = \frac{1}{\tau_0}\exp\left(-\frac{H_V^M}{k_B T}\right) \tag{3}$$

where H_V^M denotes the vacancy migration enthalpy and τ_0^{-1} a prefactor characterizing the density of vacancy sources or sinks. The solution of Equation (2) for an initial deviation $\Delta C_V(t=0) = \Delta C_V^{ini} = C_V^{ini} - C_{V,eq}$ with respect to the equilibrium concentration $C_{V,eq}(T_0)$ reads

$$C_V(t) = C_{V,eq} + \left(C_V^{ini} - C_{V,eq}\right)\exp\left(-\frac{t}{\tau}\right) \tag{4}$$

In the following, at first equilibration of vacancy concentration associated with modulation with respect to a constant temperature will be considered (Subsection 2.1) and subsequently the case of modulation upon time-linear heating (Subsection 2.2).

2.1 Equilibration of vacancy concentration associated with modulation

In order to describe vacancy equilibration associated with temperature modulation, we consider a periodic small oscillation of the temperature with amplitude $\Delta\hat{T}$ and angular frequency ω

$$T(t) = T_0 + \Delta\hat{T}\sin(\omega t) \tag{5}$$

with respect to a constant temperature T_0. Associated with the small temperature variation is a small variation in the equilibrium vacancy concentration $C_{V,eq}(T(t))$ with respect to $C_{V,eq}(T_0)$:

$$C_{V,eq}(T) = C_{V,eq}(T_0) + \left.\frac{dC_{V,eq}}{dT}\right|_{T_0}(T - T_0) \tag{6}$$

By means of the temperature-derivative of the vacancy concentration (Equation (1)).

$$\frac{dC_{V,eq}}{dT} = C_{V,eq}\frac{H_V^F}{k_B T^2} \tag{7}$$

$C_{V,eq}(T)$ (Equation (6)) can be written for $T(t)$ according to Equation (5) as

$$C_{V,eq}(T(t)) = C_{V,eq}(T_0) + C_{V,eq}(T_0)\frac{H_V^F}{k_B T_0}\frac{\Delta\hat{T}}{T_0}\sin(\omega t) \quad (8)$$

For a small temperature variation we can further neglect a variation in the equilibration rate (Equation (3)) within the modulation amplitude $\Delta\hat{T}$. This is justified for

$$\left(\frac{d\frac{1}{\tau}}{dT}\right)\Delta\hat{T} \ll \frac{1}{\tau} \quad \text{i.e.} \quad \frac{H_V^M}{k_B T}\frac{\Delta\hat{T}}{T} \ll 1 \quad (9)$$

The time behaviour of the vacancy concentration $C_V(t)$ associated with equilibration in the wake of the periodic modulation $C_{V,eq}(T(t))$ is determined by the differential equation (Equation (2)) after insertion of Equation (8):

$$\frac{dC_V(t)}{dt} + \frac{1}{\tau}\left[C_V(t) - C_{V,eq}(T_0) - C_{V,eq}(T_0)\frac{H_V^F}{k_B T_0}\frac{\Delta\hat{T}}{T_0}\sin(\omega t)\right] = 0 \quad (10)$$

or with $\Delta C_V(t) = C_V(t) - C_{V,eq}(T_0)$ and $dC_{V,eq}(T_0)/dt = 0$:

$$\frac{d\Delta C_V(t)}{dt} + \frac{\Delta C_V(t)}{\tau} = \frac{1}{\tau}C_{V,eq}(T_0)\frac{H_V^F}{k_B T_0}\frac{\Delta\hat{T}}{T_0}\sin(\omega t) \quad (11)$$

Equation (11) represents an inhomogenous differential rate equation where the right-hand side defines the driving force for concentration changes. One should emphasize that $\Delta C_V(t)$ denotes the deviation from the unmodulated value $C_{V,eq}(T_0)$ rather than from $C_{V,eq}(T)$. The inhomogeneous differential equation (Equation (11)) can be solved by the Ansatz $\Delta C_V(t) = b\sin(\omega t) + c\cos(\omega t)$, leading to the solution:

$$\Delta C_V(t) = C_{V,eq}(T_0)\frac{H_V^F}{k_B T_0}\frac{1}{\sqrt{1+\omega^2\tau^2}}\frac{\Delta\hat{T}}{T_0}\sin(\omega t + \varphi) \quad (12)$$

with the phase shift

$$\varphi = -\arctan(\omega\tau) \quad (13)$$

An essential characteristic of the solution is the phase shift between the modulation of the temperature (Equation (5)) and of the vacancy concentration (Equation (12)). This retardation is caused by the equilibration which also damps the modulation amplitude. For high equilibration rates τ^{-1}, the phase shift and the damping of the amplitude vanishes.

The analogue of the inhomogeneous differential equation (Equation (11)) in electronic circuit engineering is the series connection of a resistance R and a capacitance C with the time constant $\tau = \sqrt{RC}$, where the vacancy concentration $C_V(t)$ corresponds to the charge $Q(t)$ and where the driving force on the right-hand side is given by $C\Delta\hat{U}\sin(\omega t)$ with the modulation amplitude $\Delta\hat{U}$ of the voltage with respect to a voltage U_0. The solution of this electronic analogue fully corresponds to that given by Equations (12) and (13).[1]

2.2 Length change upon modulated time-linear heating

Based on the solution for vacancy equilibration upon modulation with respect to a constant temperature T_0 (Equation (12)), in the following the length change upon modulation during time-linear heating will be considered.

The length change associated with time-linear heating (LH) with constant heating rate R starting from temperature T_{start}:

$$T(t) = T_{start} + Rt \quad (14)$$

is composed of two parts, i.e., lattice expansion (Lat) and change of thermal vacancy concentration (Vac) (Equation (1)). The latter reads.

$$\left(\frac{\Delta L}{L_0}\right)^{LH,Vac} = \frac{1}{3}(1-r)\left(C_{V,eq}(T) - C_{V,eq}(T_{start})\right) \quad (15)$$

where r denotes the vacancy relaxation. Here, the heating rate is considered sufficiently small compared to the vacancy equilibration rate to ensure that $C_{V,eq}(T)$ is in equilibrium with respect to linear heating.

The length change due to lattice expansion reads

$$\left(\frac{\Delta L}{L_0}\right)^{LH,Lat} = \alpha_0 Rt + \frac{1}{2}\alpha_1(Rt)^2 \quad (16)$$

assuming a linear temperature dependence of the thermal coefficient of lattice expansion

$$\alpha(T) = \alpha_0 + \alpha_1 T \quad (17)$$

where the cofficients $\alpha_{0,1}$ refer to T_{start}. We note that the proper choice of the temperature dependence of α is irrelevant for the analysis method I of primary choice, presented below; the same is true for method III.

Next, the temperature modulation (mod) (Equation (5)) is superimposed to linear heating, which adds two further terms to the length change; that of lattice expansion and, the most relevant one for the present study, that

1 $\Delta Q(t) = Q(t) - Q_{eq} = \Delta Q_0/(\sqrt{1+\omega^2\tau^2})\sin(\omega t + \varphi)$ with $Q_{eq} = CU_0$ and $\Delta Q_0 = C\Delta\hat{U}$.

arising from vacancies. The modulation part from lattice expansion reads

$$\left(\frac{\Delta L}{L_0}\right)^{\mathrm{Mod,Lat}} = \alpha(T)\Delta\hat{T}\sin(\omega t) \tag{18}$$

For the length change associated with the change $\Delta C_\mathrm{V}(t)$ of vacancy concentration upon modulation, one can apply the solution above (Equation (12)), provided that the linear temperature increase within one period is small compared to the modulation amplitude, i.e.,

$$R\frac{2\pi}{\omega} \ll \hat{T} \tag{19}$$

This vacancy-associated modulated length change then reads:

$$\left(\frac{\Delta L}{L_0}\right)^{\mathrm{Mod,Vac}} = \frac{1}{3}(1-r)C_{\mathrm{V,eq}}(T)\frac{H_\mathrm{V}^\mathrm{F}}{k_\mathrm{B}T}\frac{1}{\sqrt{1+\omega^2\tau^2}} \times \frac{\Delta\hat{T}}{T}\sin(\omega t+\varphi) \tag{20}$$

with $T = T_\mathrm{start} + Rt$. The total relative length change upon modulated time-linear heating is given by the sum of the four contributions (Equations (16)–(20)):

$$\left(\frac{\Delta L}{L_0}\right) = \left(\frac{\Delta L}{L_0}\right)^{\mathrm{LH,Lat}} + \left(\frac{\Delta L}{L_0}\right)^{\mathrm{LH,Vac}} + \left(\frac{\Delta L}{L_0}\right)^{\mathrm{Mod,Lat}} + \left(\frac{\Delta L}{L_0}\right)^{\mathrm{Mod,Vac}} \tag{21}$$

This equation (Equation (21)) respresents the basis for deducing the characteristics of both thermal vacancy formation *and* equilibration from length measurements upon modulated time-linear heating, as will be pointed out in detail in the next section.

3 Analysis and discussion

3.1 Method I: high- and low-frequency measurement

In order to derive the vacancy characteristics from the measured length change (Equation (21)) upon modulated time-linear heating, the contribution from lattice expansion has to be subtracted. This is best done by means of a reference measurement at a sufficiently high frequency (HF), where the modulation is only determined by the lattice expansion, but not by vacancy equilibration, i.e., where the part $(\Delta L/L_0)_\mathrm{HF}^\mathrm{Mod,Vac}$ (Equation (20)) is neglibly small. This allows determination of the lattice expansion coefficient $\alpha(T)$ from the HF-modulated length change $(\Delta L/L_0)_\mathrm{HF}^\mathrm{Mod,Lat}$ (Equation (18)) and, in this way, subtraction of the lattice expansion contribution from the length change measured at low frequency, where modulation is both affected by thermal expansion and vacancy equilibration.

When the entire frequency-independent length change arising from thermal expansion, i.e., the sum of the linear heating Equation (16)) and the modulation part (Equation (18)), obtained from the HF measurement, is subtracted from a second length change $(\Delta L/L_0)_\mathrm{LF}$ measured at low frequency (LF), the vacancy-associated length change arising from linear heating and modulation is obtained:

$$\begin{aligned}\left(\frac{\Delta L}{L_0}\right)_\mathrm{I} &= \left(\frac{\Delta L}{L_0}\right)_\mathrm{LF} - \left(\frac{\Delta L}{L_0}\right)_\mathrm{HF}^\mathrm{LH,Lat} - \left(\frac{\Delta L}{L_0}\right)_\mathrm{HF}^\mathrm{Mod,Lat} \\ &= \left(\frac{\Delta L}{L_0}\right)_\mathrm{LF}^\mathrm{LH,Vac} + \left(\frac{\Delta L}{L_0}\right)_\mathrm{LF}^\mathrm{Mod,Vac}\end{aligned} \tag{22}$$

where the index I denotes the method I. The part of vacancy-associated length change from linear heating is

$$\left(\frac{\Delta L}{L_0}\right)_\mathrm{LF}^\mathrm{LH,Vac} = \frac{1}{3}(1-r)\left[C_{\mathrm{V,eq}}(T) - C_{\mathrm{V,eq}}(T_\mathrm{start})\right] \tag{23}$$

according to Equation (15) and that from modulation

$$\left(\frac{\Delta L}{L_0}\right)_\mathrm{LF}^\mathrm{Mod,Vac} = \frac{1}{3}(1-r)C_{\mathrm{V,eq}}(T)\frac{H_\mathrm{V}^\mathrm{F}}{k_\mathrm{B}T}\frac{1}{\sqrt{\omega^2\tau^2+1}} \times \frac{\Delta\hat{T}}{T}\sin(\omega t+\varphi) \tag{24}$$

according to Equation (20) with $T = T_\mathrm{start} + Rt$.

From Equation (22) the vacancy characteristics can be deduced as follows. The *linear heating part* (Equation (23)) of $(\Delta L/L_0)_\mathrm{I}$ directly yields the temperature variation of $C_{\mathrm{V,eq}}(T)$, from which H_V^F can be deduced as well as the temperature-independent prefactor containing the product of $(1-r)$ and $\exp\left(S_\mathrm{V}^\mathrm{F}/k_\mathrm{B}\right)$. Using the data on vacancy formation from the linear part, from the temperature-dependent *modulated part* the characteristics on vacancy migration follow. Both the amplitude (Equation (24)) and the phase angle (Equation (13)) of the modulated part depend on H_V^M and τ_0, the amplitude in addition on H_V^F, S_V^F, r.

For considering the amplitude $\hat{A}_\mathrm{I}$ of the modulated part (Equation (24)), we introduce the dimensionless inverse temperature x and the dimensionless coefficients β and γ

$$x = \frac{H_V^F}{k_B T}, \quad \beta = \frac{H_V^M}{H_V^F}, \quad \gamma = \omega\tau_0 \tag{25}$$

yielding

$$\hat{A}_I = C\frac{x^2\exp(-x)}{\sqrt{\gamma^2\exp(2\beta x)+1}} \tag{26}$$

with the temperature-independent dimensionless coefficient

$$C = \frac{1}{3}(1-r)\exp\left(\frac{S_V^F}{k_B}\right)\frac{k_B\hat{T}}{H_V^F} \tag{27}$$

3.1.1 Analysis of Method I

The modulation amplitude $\hat{A}_I$ according to Equation (26) is shown in Figure 1a in dependence of the dimensionless temperature. The amplitude increases with temperature as both the vacancy concentration and the vacancy equilibration rate are increasing. For a given temperature, $\hat{A}_I$ increases with decreasing γ, e.g., with decreasing ω, since the vacancies can equilibrate to greater extent. Correspondingly, a given amplitude is attained at lower temperature with decreasing γ. Increasing β, e.g. H_V^M, has the reverse effect, i.e., the amplitude for a given temperature decreases or else a given amplitude is reached at higher temperature.

Next, we address the choice of appropriate modulation frequency and linear heating rate.

Appropriate modulation frequency

In order that the high-frequency (HF) modulation is not affected by vacancy equilibration, which is the condition for this method, the modulation amplitude of Equation (20) associated with vacancy equilibration, for the highest applied temperature, has to be smaller than the measurement uncertainty $\Delta(\Delta L/L_0)$, i.e.,

$$\frac{1}{3}(1-r)C_{V,eq}(T)\frac{H_V^F}{k_B T}\frac{1}{\sqrt{1+\omega^2\tau^2}}\frac{\Delta\hat{T}}{T} < \Delta\left(\frac{\Delta L}{L_0}\right) \tag{28}$$

which sets a lower limit for the high frequency. Correspondingly, for the measurements at low frequency, the opposite condition is required, i.e., the amplitude has to exceed the uncertainty for the lowest applied temperature.

Appropriate linear heating rate

In order to ensure that the vacancy state is equilibrated with respect to linear heating, the associated length change $(\Delta L/L_0)^{LH,Vac}(\Delta t = \tau)$ within the characteristic time constant τ of equilibration may not exceed the measurement uncertainty $\Delta(\Delta L/L_0)$. The vacancy-associated relative length change upon time-linear heating $\Delta T = R\Delta t$ with a rate R in a time interval Δt can be obtained from the temperature-derivative of Equation (15) multiplied by ΔT, yielding:

$$\left(\frac{\Delta L}{L_0}\right)^{LH,Vac}(\Delta t) = \frac{1}{3}(1-r)C_{V,eq}(T)\frac{H_V^F}{k_B T}\frac{R\Delta t}{T} \tag{29}$$

This sets an upper limit for the heating rate R, i.e., $(\Delta L/L_0)^{LH,Vac}(\Delta t = \tau) \simeq \Delta(\Delta L/L_0)$. The upper limit must be fullfilled for the lowest temperature, where τ is highest. The condition $(\Delta L/L_0)^{LH,Vac}(\Delta t = \tau) < \Delta(\Delta L/L_0)$ is then fullfilled throughout the subsequent course of linear heating.

A lower heating rate R than that defined in this way, on the other hand, yield no gain in information, since the associated relative length change is below the detection limit, even in the low temperature regime where τ is high.

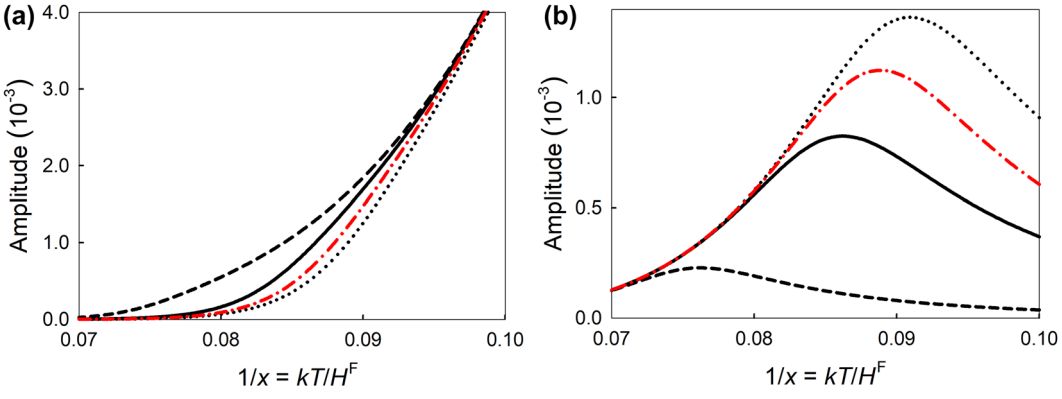

Figure 1: Modulation amplitude $\hat{A}_{I,II}$ according to Equation (26) (part a, method I) and Equation (39) (part b, method II) in dependence of dimensionless temperature $x^{-1} = (k_B T)/H_V^F$ for dimensionless parameters $C = 1$, $\beta = H_V^M/H_V^F = 1.5$ and $\gamma = \omega\tau_0 = 6.25\times10^{-8}$ (dotted line), $\gamma = 2.5\times10^{-8}$ (full line), $\gamma = 2.5\times10^{-9}$ (dashed line), as well as for $\beta = 1.55$ and $\gamma = 2.5\times10^{-8}$ (red dashed-dotted line).

Table 1: Temperature T and phase shift φ (Equation (13)) for given values of amplitude A $(\Delta L/L_0)^{\mathrm{Mod,Vac}}$ (Equation (20)) and frequency $\nu = \omega/(2\pi)$ of modulation. Parameters: Vacancy formation enthalpy $H_{\mathrm{V}}^{\mathrm{F}} = 0.42$ eV and vacancy migration enthalpy $H_{\mathrm{V}}^{\mathrm{M}} = 1.02$ eV for CuZn (see [27]), pre-exponential factor $\tau_0^{-1} = 10^8\ \mathrm{s}^{-1}$ [28], vacancy formation entropy $S_{\mathrm{V}}^{\mathrm{F}} = 2\,k_{\mathrm{B}}$, vacancy relaxation $r = 0$, temperature modulation amplitude $\hat{T} = 10$ K.

$\nu\tau_0$	2.5×10^{-10}		10^{-11}		10^{-12}	
ν (mHz)	25		1		0.1	
A	T (K)	$-\varphi$ (°)	T (K)	$-\varphi$ (°)	T (K)	$-\varphi$ (°)
10^{-6}	501	90.0	455	90.0	427	90.0
10^{-5}	542	90.0	488	89.9	459	89.8
10^{-4}	610	89.5	602	79.7	602	28.7
5×10^{-4}	835	29.5	835	1.3	835	0.1

Case example

For the sake of exemplary illustration, we consider CuZn, which exhibits a low vacancy formation enthalpy in combination with a high vacancy migration enthalpy and which, therefore, should be suited for the proposed kind of measurement. Table 1 shows the temperature T and phase shift φ (Equation (13)) for given values of amplitude A of $(\Delta L/L_0)^{\mathrm{Mod,Vac}}$ (Equation (20)) and frequencies ν of modulation based on characteristic values for vacancy formation and migration enthalpy (see [27]) and pre-exponential factor [28]. As expected, with increasing modulation frequency, the phase shift increases as well as the temperature for a given modulation amplitude. The higher the temperature, the higher is the modulation amplitude and the lower is the phase shift.

With the data set of the given example (see caption of Table 1), the minimum linear heating rate as outlined above can be derived. For $R = 10^{-3}\,\mathrm{K\,s^{-1}} = 3.6\,\mathrm{K\,h^{-1}}$ an amplitude $(\Delta L/L_0)^{\mathrm{LH,Vac}} = 10^{-6}$ is obtained from Equation (29) for $T = 480$ K, i.e., this value R represents the lower limit, if 10^{-6} is considered as experimental uncertainty and 480 K the minimum temperature. This value of R well fullfills the condition (Equation (19))

$$R\frac{2\pi}{\omega} = R\frac{1}{\nu} = 1\,\mathrm{K} \ll \hat{T} = 10\,\mathrm{K} \tag{30}$$

of the example for the frequency of $\nu = 1$ mHz. Also the condition according to Equation (9) is fairly well fullfilled. For $T = 500$ K, a value of

$$\frac{H_{\mathrm{V}}^{\mathrm{M}}}{k_{\mathrm{B}}T}\frac{\Delta\hat{T}}{T} = 0.47 \tag{31}$$

is obtained and correspondingly lower values for higher temperatures.

3.2 Method II: measurement without high-frequency approach

When the HF-approach as used for method I is not taken into consideration, the length change associated with lattice expansion α *cannot* be obtained from the modulation. An alternative way in this case is to determine an expansion coefficient

$$\alpha_{\mathrm{LH}}(T) = \frac{\mathrm{d}}{\mathrm{d}T}\left(\frac{\Delta L}{L_0}\right)^{\mathrm{LH}} \tag{32}$$

from the length change part $(\Delta L/L_0)^{\mathrm{LH}}$ of linear heating and to obtain a difference curve corresponding to Equation (22), but for the same frequency.

However, the linear heating part and, therefore, $\alpha_{\mathrm{LH}}(T)$ is not simply given by the lattice expansion coefficient

$$\frac{\mathrm{d}}{\mathrm{d}T}\left(\frac{\Delta L}{L_0}\right)^{\mathrm{LH,Lat}} = \alpha(T) = \alpha_0 + \alpha_1 T \tag{33}$$

but is the sum of Equation (33) and the temperature-derivative $(\mathrm{d}/\mathrm{d}T)(\Delta L/L_0)^{\mathrm{LH,Vac}}$ from the vacancy contribution (Equation (15)). Subtracting the length change $\alpha_{\mathrm{LH}}(T)(Rt + \hat{T}\sin(\omega t))$ deduced in this way from the measured length change $(\Delta L/L_0)$ yields the difference curve for this method II:

$$\left(\frac{\Delta L}{L_0}\right)_{\mathrm{II}} = -\frac{1}{2}\alpha_1(Rt)^2 + \left(\frac{\Delta L}{L_0}\right)^{\mathrm{Mod,\,Vac}} - \frac{\mathrm{d}}{\mathrm{d}T}\left(\frac{\Delta L}{L_0}\right)^{\mathrm{LH,\,Vac}}\Delta\hat{T}\sin(\omega t) \tag{34}$$

where the summand $-1/2\alpha_1(Rt)^2$ arises from

$$\frac{\mathrm{d}}{\mathrm{d}T}\left(\frac{\Delta L}{L_0}\right)^{\mathrm{LH,Lat}} Rt = \left(\frac{\Delta L}{L_0}\right)^{\mathrm{LH,Lat}} + \frac{1}{2}\alpha_1(Rt)^2 \tag{35}$$

For $(\Delta L/L_0)_{\mathrm{II}}$ (Equation (34)) follows with Equation (15):

$$\left(\frac{\Delta L}{L_0}\right)_{\mathrm{II}} = -\frac{1}{2}\alpha_1(Rt)^2 + \frac{1}{3}(1-r)C_{\mathrm{V,eq}}(T)\frac{H_{\mathrm{V}}^{\mathrm{F}}}{k_{\mathrm{B}}T}\frac{\Delta\hat{T}}{T} \times\left(\frac{1}{\sqrt{1+\omega^2\tau^2}}\sin(\omega t+\varphi) - \sin(\omega t)\right) \tag{36}$$

and after trigonometric transformations

$$\left(\frac{\Delta L}{L_0}\right)_{\mathrm{II}} = -\frac{1}{2}\alpha_1(Rt)^2 - \frac{1}{3}(1-r)C_{\mathrm{V,eq}}(T)\frac{H_{\mathrm{V}}^{\mathrm{F}}}{k_{\mathrm{B}}T} \times\sqrt{\frac{\omega^2\tau^2}{1+\omega^2\tau^2}}\frac{\Delta\hat{T}}{T}\sin(\omega t+\phi) \tag{37}$$

with the phase shift

$$\phi = \arctan\left(\frac{1}{\omega\tau}\right) \tag{38}$$

and with $T = T_{\text{start}} + Rt$.

Note that in this case of method II, the difference (Equation (34)) is obtained from one and the same heating curve, in contrast to method I where the difference of two curves measured for low and high frequency is taken. However, the result (Equation (37)) of method II also contains a contribution from the lattice expansion $(-1/2\alpha_1(Rt)^2)$, in contrast to method I. Since this is a non-oscillating contribution it can easily be subtracted from the oscillating part and, therefore, will not be considered in the following.

Rewriting the amplitude $\hat{A}_{\text{II}}$ of Equation (37) in dimensionless quantities (Equations (25) and (27)) as for method I (Equation (26)), yields

$$\hat{A}_{\text{II}} = Cx^2 \exp(-x)\sqrt{\frac{\gamma^2 \exp(2\beta x)}{\gamma^2 \exp(2\beta x) + 1}} \tag{39}$$

The temperature variation of the amplitude of Equation (37) exhibits an extremum which can be deduced from the implicit equation:

$$T_{\text{ext}} = \frac{1}{2}\left(\frac{H_{\text{V}}^{\text{F}}}{k_{\text{B}}} - \frac{H_{\text{V}}^{\text{M}}}{k_{\text{B}}}\frac{1}{\omega^2\tau^2(T_{\text{ext}}) + 1}\right) \tag{40}$$

For graphical solution, Equation (40) can be rewritten with the dimensionless quantities (Equation (25)) as follows:

$$\frac{1}{\beta} - \frac{2}{\beta x} = \frac{1}{\gamma^2 \exp(2\beta x) + 1} \tag{41}$$

From Equation (37) the vacancy characteristics (H_{V}^{F}, S_{V}^{F}, r, H_{V}^{M}, and τ_0) can be deduced. As for method I, both the amplitude and the phase angle (Equation (38)) of the modulated part depend on H_{V}^{M} and τ_0, the amplitude in addition on H_{V}^{F}, S_{V}^{F}, r. However, in contrast to method I (Equation (23)), here the part from vacancy formation cannot be separately obtained from the linear heating part. Therefore, although Equation (37) for a given ω principally contains the entire information, in practice, measurements for at least two frequencies are necessary.

3.2.1 Analysis of Method II

The modulation amplitude according to Equation (39) is shown in Figure 1b in dependence of the dimensionless temperature. Striking differences compared to the amplitude of method I are the occurence of a maximum and the reversed variation with the parameters β and γ (compare Figure 1a and b). This is due to the different square-root term of $\hat{A}_{\text{II}}$ compared to $\hat{A}_{\text{I}}$ (Figure 2).

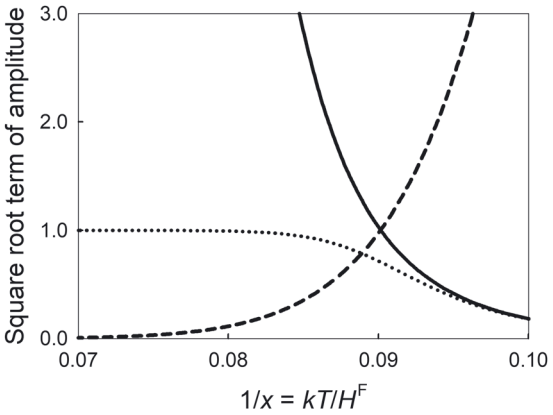

Figure 2: Square root term of $\hat{A}_{\text{I}}$ according to Equation (26) $(1/(\gamma^2 \exp(2\beta x) + 1)^{1/2})$ (dashed line), of $\hat{A}_{\text{II}}$ according to Equation (39) $\left(\left[\gamma^2 \exp(2\beta x)/\{\gamma^2 \exp(2\beta x) + 1)\}\right]^{1/2}\right)$ (dotted line) and ratio $\hat{A}_{\text{II}}/\hat{A}_{\text{I}}$ $(\gamma \exp(\beta x))$ (full line) in dependence of dimensionless temperature $x^{-1} = (k_{\text{B}}T)/H_{\text{V}}^{\text{F}}$ for dimensionless parameters $\beta = H_{\text{V}}^{\text{M}}/H_{\text{V}}^{\text{F}} = 1.5$, $\gamma = \omega\tau_0 = 2.5 \times 10^{-8}$, and $C = 1$.

Towards low temperatures $\hat{A}_{\text{II}}$ decreases for the same reason as for method I, namely the decreasing vacancy concentration C_{V}. A maximum value arises for method II, since in that case the difference $(\Delta L/L_0)_{\text{II}}$ (Equation (37)) also goes to zero for high temperatures. This is the case for $\omega\tau \to 0$, i.e., $\omega \ll \tau^{-1}$, when the equilibration rate is high, i.e., when C_{V} is always in equilibrium, or either when ω is low. Correspondingly, $\hat{A}_{\text{II}}$ decreases in this regime with increasing temperature (i.e., increasing equilibration rate) and, for given T, with decreasing γ (e.g., ω). The lower γ is, the lower is the temperature where the decrease of $\hat{A}_{\text{II}}$ sets in with increasing T (see shift of maximum), which also becomes evident from Equation (40). Lowering of β, e.g., of H_{V}^{M}, causes a similar trend as a decrease of ω, due to the concomitant increase in the equilibration rate. Figure 2 underlines that the high-temperature decrease in $\hat{A}_{\text{II}}$ arises from its square-root factor, which in contrast to method I, decreases with increasing T.

A further remarkable difference to method I is the behaviour for large values of $\omega\tau$, i.e., for $\omega \gg \tau^{-1}$, when either ω is high or the equilibration occurs slowly. Here, for method I the amplitude (Equation (24)), which is the difference to the high-frequency part, goes to zero. For method II, the square-root term $(\omega^2\tau^2)/(1 + \omega^2\tau^2)$ in Equation (37) approaches one and the phase angle ϕ (Equation (38)) zero. In that case only the second sine-function $(-\sin(\omega t))$ (Equation (36)) remains for $(\Delta L/L_0)_{\text{II}}$. This is because

$\alpha_{LH}(T)$, contains only the unmodulated contribution from vacancies. Therefore, the function $-\sin(\omega t)$ in the difference, where $\alpha_{LH}(T)T(t)$ is subtracted (Equation (36)), takes into account the deviation of C_V from the unmodulated value upon modulation.

In summary, one may state that although method II yields access to the characteristics of vacancy formation and equilibration to the same extent as method I, the latter high-frequency approach, if applicable, should be preferred as the less laborious way.

3.3 Method III: Modulation after step-like temperature change

The application of the modulation technique is not restricted to time-linear heating, but may also be used to monitor isothermal vacancy equilibration after step-like temperature change.

The standard solution according to Equation (4) gives the isothermal length change as answer to an initial step-like change of the equilibrium vacancy concentration

$$\Delta C_V^{ini} = \Delta C_V(t=0) = C_{V,eq}(T_{ini}) - C_{V,eq}(T_0) \qquad (42)$$

that is caused by temperature jump from T_{ini} to T_0. The solution with temperature modulation $T = T_0 + \Delta\hat{T}\sin(\omega t)$ after step-like temperature change is given by simply adding the inhomogeneous solution (Equation (12)), which yields

$$\Delta C_V(t) = \left(C_{V,eq}(T_{ini}) - C_{V,eq}(T_0)\right)\exp\left(-\frac{t}{\tau}\right) + C_V(T_0)\frac{H_V^F}{k_B T_0}\frac{1}{\sqrt{1+\omega^2\tau^2}}\frac{\Delta\hat{T}}{T_0}\sin(\omega t+\varphi) \qquad (43)$$

with the corresponding length change

$$\left(\frac{\Delta L}{L_0}\right) = \frac{1}{3}(1-r)\Delta C_V(t) + \alpha(T_0)\Delta\hat{T}\sin(\omega t) \qquad (44)$$

where φ denotes the phase shift (Equation (13)) and α the thermal expansion coefficient of the lattice.

As for method I, the contribution from thermal lattice expansion can be separately obtained from a measurement at high frequency, where vacancy equilibration does not contribute to modulation. Compared to the static isothermal case (Equation (4)), in the modulation case (Equation (43)) the characteristic vacancy equilibration rate τ^{-1} cannot just be derived from the exponential decay but also from the modulation amplitude and the phase shift which improves the accuracy.

Table 2: Vacancy formation enthalpy H_V^F and vacancy migration enthalpy H_V^M in B2 intermetallic alloys. The activation energy of self-diffusion Q^{SD} is given, when H_V^M is deduced from $Q^{SD} - H_V^F$.

	H_V^F (eV)	H_V^M (eV)	Q^{SD} (eV)
$Fe_{55}Al_{45}$	1.0 [21]	1.5 [21]	
$Ni_{47}Al_{53}$	1.5 [21]	1.8 [21]	
PdIn	0.41 [29]	1.9	2.3 [30]
CuZn	0.42 (see [27])	1.02	1.56 (see [27])

4 Concluding remarks

The major advantages of the presented modulation technique compared to static isothermal measurements after temperature jumps can be summarized as follows:

1. Thermal vacancy formation and equilibration are monitored under quasi-equilibrium conditions avoiding obstacles associated with fast temperature changes.
2. Principally the entire vacancy characteristics are included in one $(\Delta L/L_0)(t)$-curve measured upon a single modulated linear-heating sequence provided heating rate and modulation frequency are estimated appropriately in advance. The contribution from thermal lattice expansion can unambiguously be determined from a reference measurement at high modulation frequencies.
3. In contrast to the static isothermal case, the modulation yields access to the phase shift (Equation (13)) between $(\Delta L/L_0)(t)$ and $T(t)$. This yields additionally most direct information on the equilibration time constant τ, which can be determined in this way more reliably compared to the static case where this is obtained from the time-exponential decay (Equation (4)). It should be mentioned, however, that after temperature jump the equilibration of a high excess concentration of vacancies can be monitored which, on the other hand, can be favourable compared to the present method in the range where the equilibrium vacancy concentration is still low.

Best suited to exploring the potentials of the proposed method appear to be intermetallic alloys with B2-type structure, which exhibit low H_V^F- and high H_V^M-values. Among those are the ones listed in the following table: FeAl, NiAl [21], PdIn [29, 30], and CuZn (see [27]) (Table 2).

Acknowledgements: This work was performed in the framework of the interuniversity cooperation of TU Graz

and Univ. Graz on natural sciences (NAWI Graz). The authors are indebted to Peter Schlosser, Institute of Applied Mathematics, TU Graz, for fruitful discussion.

Author contributions: All the authors have accepted responsibility for the entire content of this submitted manuscript and approved submission.

Research funding: None declared.

Conflict of interest statement: The authors declare no conflicts of interest regarding this article.

References

1. Fizeau M. H. *Ann. Chem. Phys.* 1864, *4*, 143.
2. Edmonds D. The strengthening of an Fe-V-C low-alloy steel by carbide precipitation during continuous cooling from the austenitic condition. *Metall. Trans.* 1973, *4*, 2527–2533. https://doi.org/10.1007/BF02644254.
3. Recarte V., Pérez-Sáez R., No M., Juan S. Dilatometric study of the precipitation kinetics in Cu-Al-Ni shape memory alloys. *J. Phys. IV France* 1997, *07*, C5–329–C5–334. https://doi.org/10.1051/jp4:1997552.
4. Garcia-Mateo C., Caballero F., Capdevila C., de Andres C. G. Estimation of dislocation density in bainitic microstructures using high-resolution dilatometry. *Scripta Mater.* 2009, *61*, 855–858. https://doi.org/10.1016/j.scriptamat.2009.07.013.
5. Lasagni F., Dumont M., Salamida C., Acuna J., Degischer H. P. Dilatometry revealing Si precipitation in AlSi-alloys. *Int. J. Mater. Res.* 2009, *100*, 1005–1013. https://doi.org/10.3139/146.110145.
6. Daoudi M. I., Triki A., Redjaimia A., Yamina C. The determination of the activation energy varying with the precipitated fraction of metastable *β*'' phase in an Al-Mg-Si alloy using non-isothermal dilatometry. *Thermochim. Acta* 2014, *577*, 5–10. https://doi.org/10.1016/j.tca.2013.12.007.
7. Milkereit B., Reich M., Kessler O. Detection of quench induced precipitation in Al alloys by dilatometry. *Mater. Sci. Forum* 2017, *877*, 147–152. https://doi.org/10.4028/www.scientific.net/msf.877.147.
8. Luckabauer M., Sprengel W., Würschum R. A high-stability non-contact dilatometer for low-amplitude temperature-modulated measurements. *Rev. Sci. Instrum.* 2016, *87*, 075116. https://doi.org/10.1063/1.4959200.
9. Hengge E., Enzinger R., Luckabauer M., Sprengel W., Würschum R. Quantitative volumetric identification of precipitates in dilute alloys using high-precision isothermal dilatometry. *Phil. Mag. Lett.* 2018, *98*, 301–309. https://doi.org/10.1080/09500839.2018.1542170.
10. Enzinger R., Hengge E., Sprengel W., Würschum R. High-precision isothermal dilatometry as tool for quantitative analysis of precipitation kinetics: case study of dilute Al alloy. *J. Mater. Sci.* 2019, *54*, 5083–5091. https://doi.org/10.1007/s10853-018-03210-z.
11. Würschum R., Enzinger R., Hengge E., Sprengel W. Recent progress in dilatometry for quantitative analysis of precipitation kinetics. *IOP Conf. Ser. Mater. Sci. Eng.* 2019, *580*, 012502. https://doi.org/10.1088/1757-899X/580/1/012052.
12. Steyskal E.-M., Oberdorfer B., Sprengel W., Zehetbauer M., Pippan R., Würschum R. Direct experimental determination of grain boundary excess volume in metals. *Phys. Rev. Lett.* 2012, *108*, 055504. https://doi.org/10.1103/PhysRevLett.108.055504.
13. Oberdorfer B., Setman D., Steyskal E.-M., Hohenwarter A., Sprengel W., Zehetbauer M., Pippan R., Würschum R. Grain boundary excess volume and defect annealing of copper after high-pressure torsion. *Acta Mater.* 2014, *68*, 189–195. https://doi.org/10.1016/j.actamat.2013.12.036.
14. Kotzurek J. A., Steyskal E.-M., Oberdorfer B., Hohenwarter A., Pippan R., Sprengel W., Würschum R. Direct measurement of vacancy relaxation by dilatometry. *Appl. Phys. Lett.* 2016, *109*, 021906. https://doi.org/10.1063/1.4958895.
15. Kotzurek J. A., Sprengel W., Krystian M., Simic S., Pölt P., Hohenwarter A., Pippan R., Würschum R. Structural anisotropy in equal-channel angular extruded nickel revealed by dilatometric study of excess volume, internat. *J. Mater. Res.* 2017, *108*, 81–88. https://doi.org/10.3139/146.111463.
16. Enzinger R., Neubauer C., Kotzurek J., Sprengel W., Würschum R. Kinetics of vacancy annealing upon time-linear heating applied to dilatometry. *J. Mater. Sci.* 2018, *53*, 2758–2765. https://doi.org/10.1007/s10853-017-1780-4.
17. Feder R., Nowick A. S. Use of thermal expansion measurements to detect lattice vacancies near the melting point of pure lead and aluminum. *Phys. Rev.* 1958, *109*, 1959–1963. https://doi.org/10.1103/PhysRev.109.1959.
18. Simmons R., Balluffi R. Measurements of equilibrium vacancy concentrations in aluminum. *Phys. Rev.* 1960, *117*, 52–61. https://doi.org/10.1103/PhysRev.117.52.
19. Hehenkamp T., Berger W., Kluin J.-E., Lüdecke C., Wolff J. Equilibrium vacancy concentrations in copper investigated with the absolute technique. *Phys. Rev. B* 1992, *45*, 1998–2003. https://doi.org/10.1103/PhysRevB.45.1998.
20. Van Ommen A., Miranda J. A dilatometric study of vacancy mobility in the intermetallic compound CoGa. *Phil. Mag.* 1981, *43*, 387–407. https://doi.org/10.1080/01418618108239417.
21. Schaefer H.-E., Frenner K., Würschum R. Time-differential length change measurements for thermal defect investigations: intermetallic *B*2-FeAl and *B*2-NiAl compounds, a case study. *Phys. Rev. Lett.* 1999, *82*, 948–951. https://doi.org/10.1103/PhysRevLett.82.948.
22. James J., Spittle J., Brown S., Evans R. A review of measurement techniques for the thermal expansion coefficient of metals and alloys at elevated temperatures. *Meas. Sci. Technol.* 2001, *12*, R1–R15. https://doi.org/10.1088/0957-0233/12/3/201.
23. Kraftmakher Y. Modulation calorimetry and related techniques. *Phys. Rep.* 2002, *356*, 1–117. https://doi.org/10.1016/S0370-1573(01)00031-X.
24. Kamasa P., Myslinski P., Staskiewicz J. Instantaneous coefficient of thermal expansion determined by temperature-modulated dilatometry. *Czech. J. Phys.* 2004, *54*, D627–D630. https://doi.org/10.1007/s10582-004-0159-3.

25. Kamasa P., Myslinski P., Pyda M. Experimental aspects of temperature-modulated dilatometry of polymers. *Thermochim. Acta* 2006, *442*, 48–51. https://doi.org/10.1016/j.tca.2005.11.017.
26. Myslinski P. Investigation of the thermal stability of hard coatings by modulated temperature dilatometry. *Vacuum* 2008, *83*, 757–760. https://doi.org/10.1016/j.vacuum.2008.05.006.
27. Schaefer H. E., Badura-Gergen K. Systematics of thermal defect formation, migration and of self-diffusion in intermetallic compounds. *Defect Diff. Forum* 1997, *143*, 193–208. https://doi.org/10.4028/www.scientific.net/DDF.143-147.193.
28. Würschum R., Grupp C., Schaefer H.-E. Simultaneous study of vacancy formation and migration at high temperatures in B2-type Fe aluminides. *Phys. Rev. Lett.* 1995, *75*, 97–100. https://doi.org/10.1103/PhysRevLett.75.97.
29. Jiang C., Chen L.-Q., Liu Z.-K. First-principles study of constitutional and thermal point defects in B2 PdIn. *Intermetallics* 2006, *14*, 248–254. https://doi.org/10.1016/j.intermet.2005.05.012.
30. Hahn H., Frohberg G., Wever H. Self diffusion in the intermetallic B2 electron compound PdIn. *phys. stat. sol. (a)* 1983, *79*, 559–565. https://doi.org/10.1002/pssa.2210790229.